applied sciences

MDPI

Article

Investigation of Gentamicin Release from Polydopamine Nanoparticles

Rahila Batul [1,2], Abdul Khaliq [3], Ahmed Alafnan [2], Mrinal Bhave [1] and Aimin Yu [1,*]

[1] Department of Chemistry and Biotechnology, Swinburne University of Technology, Hawthorn, VIC 3122, Australia; r.batool@uoh.edu.sa (R.B.); mbhave@swin.edu.au (M.B.)
[2] Department of Pharmacology and Toxicology, College of Pharmacy, University of Ha'il, Ha'il 55211, Saudi Arabia; a.alafnan@uoh.edu.sa
[3] Department of Mechanical Engineering, College of Engineering, University of Ha'il, Ha'il 55211, Saudi Arabia; ab.ismail@uoh.edu.sa
* Correspondence: aiminyu@swin.edu.au

Abstract: Polydopamine (PDA), being highly reactive in nature, has acquired great attention in multi-disciplinary fields. Owing to its fascinating properties, including its biocompatible, non-toxic and readily bio-degradative nature, we investigated the drug loading and release behavior, using an aminoglycoside antibiotic gentamicin (G) as a model drug. The gentamicin was loaded into the PDA nanoparticles (NPs) via an in situ polymerization method. The release kinetics of the gentamicin was then studied in pH 3, 5 and 7.4. Two batches with varied gentamicin loadings, G-PDA NPs 1:1 (with approx. 84.1% loaded gentamicin) and G-PDA NPs 0.6:1 (with approx. 72.7% loaded gentamicin), were studied. The drug release data were analyzed by LC–MS. The PDA showed good stability in terms of gentamicin release at alkaline pH over a period of seven days. The negative surface charge of PDA at pH 7.4 makes a strong bond with gentamicin, hence preventing its release from the PDA NPs. However, at pH 5 and 3, the amine groups of PDA are more prone towards protonation, making PDA positively charged, hence the repulsive forces caused the gentamicin to detach and release from the G-PDA NPs. Consequently, approx. 40% and 55% drug release were observed at pH 5 and 3, respectively, from the G-PDA NPs 1:1. However, the drug released from G-PDA NPs 0.6:1 was found to be one half as compared to the G-PDA NPs 1:1, which is obvious to the concentration gradient. These findings suggested that the in situ loading method for gentamicin could provide drug release over a period of seven days, hence defending the drug's efficacy and safety challenges. Furthermore, two kinetic models, namely the Ritger–Peppas and Higuchi models, were implemented to determine the drug release kinetics. Curve fitting analysis supported our findings for the drug release kinetics which are followed by PDA structural changes in response to pH.

Keywords: polydopamine; drug delivery; gentamicin; drug release kinetics; kinetic models

check for updates

Citation: Batul, R.; Khaliq, A.; Alafnan, A.; Bhave, M.; Yu, A. Investigation of Gentamicin Release from Polydopamine Nanoparticles. *Appl. Sci.* **2022**, *12*, 6319. https://doi.org/10.3390/app12136319

Received: 16 May 2022
Accepted: 16 June 2022
Published: 21 June 2022

Publisher's Note: MDPI stays neutral with regard to jurisdictional claims in published maps and institutional affiliations.

Copyright: © 2022 by the authors. Licensee MDPI, Basel, Switzerland. This article is an open access article distributed under the terms and conditions of the Creative Commons Attribution (CC BY) license (https://creativecommons.org/licenses/by/4.0/).

1. Introduction

Nano-based drug delivery systems have received remarkable attention in the past few decades in various biomedical disciplines, including medical biology, diagnosis, prevention and remediation of diseases [1,2]. A considerable number of nanoparticles have been investigated so far, for the delivery of drugs and other biomolecules in a controlled manner to their specific targeted sites [3,4]. Some of these drug-loaded NPs are in clinical use for the treatment of various life-threatening disorders, particularly cancers [5,6]. However, there is still a continuous demand for exploring such NPs to improve the quality of life. Since 2007, PDA NPs have gained extensive attention from researchers all over the world in several fields of life [7,8]. The main reasons for the interest in PDA NPs are attributed to their highly reactive nature, as well as their availability in various forms and shapes, including nanocapsules, nanoparticles, nanocoatings and core-shell nanocomposites [9,10]. The concept of PDA was conceived by researchers from the amine-assisted catechol moieties, lysine and

3,4-dihydroxyphenylalanine (DOPA), found in marine mussels and mainly responsible for their super adherence on diverse surfaces [11]. From this discovery, Messersmith et al. investigated the DOPA derivative, dopamine hydrochloride, which carries both of the amine and catechol functional moieties, thereby, responsible for coating diverse substrates in mild alkaline conditions [11,12]. The dopamine undergoes self-polymerization, hence giving rise to various forms of PDA, depending on specific method conditions. Of all of these methods, the solution oxidation method was found to be versatile, convenient, reproductive and cost-effective [13,14]. However, minor modifications, in terms of polymerization time and type of reactants, could be tailored depending on the required morphology and/or form of PDA. Researchers are still investigating new methods of PDA synthesis with certain modifications [10,15]. Recently, Salima and Vincent published their review illustrating various methods reported so far, for PDA synthesis and its structural derivatives [16]. Moreover, structural analogues of PDA and its properties are still not clear, hence are under investigation by several researchers, since its discovery in 2005 [17–19]. Recently, Islam et al. also reported various synthetic methods and formation mechanisms of PDA [20].

Based on its highly reactive nature, PDA exhibits an outstanding and wide variety of properties, such as intensive light absorption in the UV-visible range, photothermal conversion efficiency, metal chelating ability, as a reducing agent, super-magnetism, opto-electric properties, as a photoacoustic agent, biosensor, photocatalyst, chemotherapeutic and other physicochemical characteristics. Consequently, PDA has emerged significantly in every field of research [20–24]. Moreover, based on its biocompatible, biodegradable and non-toxic nature, we have aimed in our work to determine the loading and release kinetics of an aminoglycoside antibiotic, i.e., gentamicin as a model drug. Gentamicin is used to treat various types of bacterial infections. However, some clinicians have limited its use because of its limited bioavailability, toxicity, shorter half-life and low intestinal absorption. Therefore, the nano-formulation approach may be helpful to overcome such challenges [25,26].

In a recent work, we reported on the synthesis of PDA NPs and gentamicin loading using an in situ polymerization method [14,27]. We particularly investigated an in situ method for drug loading to overcome the problems encountered with other loading methods, including the use of toxic substances during synthesis; increased labor and time; and premature and uncontrolled drug release. These drawbacks ultimately lead to drug instability and efficacy, hence compromising the actual purpose of loading drugs into NPs [28–30].

Our findings also suggested that PDA exhibits a very capacious nature, providing benefits for a high loading efficiency of approx. 84% for gentamicin. Moreover, antimicrobial testing has also been reported for as-prepared particles against two microbial species Gram (+) *Staphylococcus aureus* and Gram (–) *Pseudomonas aeruginosa* to determine antimicrobial efficiencies.

In a continuation of our previous work, here we present the quantification of gentamicin release over an extended period, using the dialysis method. An in vitro release test was performed for two batches with varied gentamicin-loading amounts (G-PDA NPs 1:1 and G-PDA NPs 0.6:1) at three pH conditions: 3; 5 and 7.4. The drug release quantification was carried out by liquid chromatography–mass spectrometry (LC–MS). Furthermore, the drug release profiles were thoroughly investigated by implementing mathematical models. Two kinetic models, namely the Ritger–Peppas and Higuchi models, were found to be best suited, as revealed by the high correlation R^2 values. The curve fitting analysis further supported the pH-dependent drug release kinetics. Our findings suggested that pH-responsive drug release would prevent the premature release of gentamicin, hence retaining the drug's efficiency and safety.

2. Materials and Methodology

2.1. Materials

The dopamine hydrochloride, ammonia aqueous solution (NH_3 content: 38–40%) and ethanol were purchased from Sigma-Aldrich (Sigma-Aldrich Pty. Ltd., Sydney, NSW, Australia). The gentamicin sulfate (active fraction: 590 µg gentamicin/mg) was obtained from AK Scientific (Union City, CA, USA). The sodium chloride (NaCl), monobasic sodium phosphate (NaH_2PO_4), dibasic sodium phosphate (Na_2HPO_4), concentrated sulfuric acid, 30% hydrogen peroxide chromatography grade acetonitrile, ammonium formate and formic acid were purchased from Sigma-Aldrich (Sigma-Aldrich Pty. Ltd., Sydney, NSW, Australia). The hydrochloric acid (HCl) and sodium hydroxide (NaOH) pellets were purchased from Sigma-Aldrich (Sigma-Aldrich Pty. Ltd., Sydney, NSW, Australia).

The Tris buffer (10 mM; pH 8.5), prepared by dissolving Tris base and pH, was adjusted with 1 M hydrochloric acid (HCl). The phosphate buffer solutions (PBS) with different pH were made by mixing the solutions of NaH_2PO_4 with Na_2HPO_4 and the desired pH was adjusted using HCl and/or NaOH solutions. The SnakeSkin™ dialysis tubing, with a 3500 molecular weight cut-off (MWCO) and 22 mm dry diameter, was purchased from Thermo Scientific (Waltham, MA, USA). The chemicals used in all of the experiments were of analytical grade and applied without further purification. The Milli-Q water (fitted with a Millipak® 40 filter unit), having a resistivity of 18.2 MΩ cm, was employed in all of the experiments.

2.2. Synthesis of Gentamicin-Loaded Polydopamine Nanoparticles (G-PDA NPs)

The G-PDA NPs were prepared by using the in situ polymerization method, as mentioned in our previous published work. Various batches were prepared by varying the amount of gentamicin (50 mg, 75 mg, 100 mg and 125 mg) in the reaction mixture and keeping the amount of dopamine constant (i.e., 125 mg). Hence, for identifying the batches in terms of weight ratios, they are named as G-PDA NPs 0.4:1, G-PDA NPs 0.6:1, G-PDA NPs 0.8:1 and G-PDA NPs 1:1, respectively [27]. The physical characterization of the as-prepared particles was carried out by hydrodynamic particle size, morphology and Zeta potential analysis. Furthermore, the chemical interaction between the PDA and gentamicin was studied through XPS, which was well documented in our previous work [27].

2.3. Investigation of Gentamicin Loading in G-PDA NPs

The quantification of the gentamicin loading in PDA NPs was determined by using supernatants obtained after centrifugation of the drug-loaded NPs. The supernatants were analyzed via Liquid Chromatography–Mass Spectrometry (LC–MS) to determine the unloaded amount of gentamicin. Hence, it would indirectly indicate the % of loaded drug in the PDA NPs. For detailed methodology, please refer to our article [27].

2.4. Investigation of Gentamicin Release from G-PDA NPs

The gentamicin release from the G-PDA NPs was determined through the dialysis method. For this purpose, a dispersion of 10 mg/mL of the G-PDA NPs was poured into the dialysis tubing. An amount of 1 mL of 10 mg/mL of the G-PDA NPs was poured in a 3.5 kDa dialysis tube and dialyzed against 15 mL of PBS (0.1 M) at different pH (7.4, 5 and 3), respectively. The temperature was maintained at 37 °C throughout the experiment. At predetermined time intervals, 1.5 mL of release medium was taken and replaced by the same quantity of fresh buffer. The amount of released gentamicin was measured via LC–MS. The concentration of the dialysis solution was determined from a derived calibration curve of standard gentamicin solution from 0.1, 0.5, 1 and 1.5 µg/mL. Both cumulative and non-cumulative plots were made to study the drug release profile. Each drug release experiment was repeated three times by maintaining all of the experimental conditions.

The instrumental conditions used for LC–MS to determine the drug release rate are shown in Table 1:

Table 1. Elements and experimental conditions of LC–MS.

Elements of LC–MS Used	Experimental Conditions
Instrument	Xevo TQS micro with Acquity UPLC 100
Column	Waters Ethylene Bridged Hybrid (BEH) C18
Column size	2.1 mm ID × 50 mm length
Particle size	1.7 µm
Eluent	20 mM Heptafluorobutyric acid (HFBA) in 70:30 Water: Acetonitrile
Flow rate	0.5 mL/min
Injection volume	0.5 µL
Detection	MRM in positive mode

Furthermore, to determine the drug release rate, kinetic analysis of drug release profiles was also carried out, by fitting the mathematical models.

3. Results and Discussion

3.1. Gentamicin Loading in PDA NPs

The gentamicin loading in the PDA NPs was successfully accomplished by an in situ polymerization method. The detailed characterization of the G-PDA NPs was carried out by particle size analyzer, Zeta sizer, SEM and FTIR in detail in our previous work. The particle size was increased by increasing the concentration of gentamicin in the reaction mixture, proved by SEM and hydrodynamic particle size analysis. Because of the positively charged amine groups of gentamicin, the particle Zeta potential values were tending to neutralize after the drug loading. It might indicate the possibility of positive–negative chemical interaction present between the positively charged amine groups of the gentamicin and the negatively charged hydroxyl groups of the PDA at a working pH of 12.5. The FTIR analysis also presented some chemical shifts and peak intensities of the hydroxyl and amine groups, demonstrating a chemical interaction between the molecules. The chemical interaction mechanism of the gentamicin and PDA was also studied in detail using XPS, which provides evidence of hydrogen bonding present between the amine groups of gentamicin and hydroxyl groups of PDA [27].

It was found that the PDA could load gentamicin in ascending order with a sequential increase in the feeding amount of gentamicin, while keeping the concentration of dopamine constant. Consequently, the PDA could possibly carry approximately 84% of gentamicin at 1:1 ratio of gentamicin to dopamine.

Further details regarding the morphology, chemical interaction between gentamicin and PDA and antimicrobial efficacy of the G-PDA NPs have already been reported in our work [27].

3.2. In Vitro Drug Release from G-PDA NPs

The pH-responsive drug release for gentamicin was investigated for two batches viz.; G-PDA NPs 1:1 and G-PDA NPs 0.6:1 against three pH values, i.e., 7.4, 5 and 3. The release profile of gentamicin was determined from the LC–MS. The concentrations of the drug release were obtained through a calibration curve of standard gentamicin, as shown in Figure S1 (Supplementary Materials). The standard gentamicin peaks were also obtained from all three of the isomers C1a, C2/C2a and C1, respectively, at their corresponding m/z values as shown in Figures S2–S4 (Supplementary Materials).

An ideal drug-loaded nanocarrier normally shows a release-inhibition phenomenon at physiological pH and becomes free to release the bound drug only when and where bacterial multiplication takes place, thus decreasing the local pH in the vicinity. Based on this concept, three pH conditions were studied for the drug release from the G-PDA NPs. Notably, the PDA's zwitterionic nature allows it to substitute surface charge at variable pH

conditions [28]. Therefore, PDA should block the release of aminoglycosides in normal physiological conditions because of its negatively charged surface at alkaline pH. During bacterial colonization on the surface, the local acidification induced by bacterial metabolism should change the structural properties of PDA, due to the protonation of the amine groups, hence accelerating the release of the gentamicin from the G-PDA NPs.

To investigate the pH-dependent drug release of G-PDA 1:1 and 0.6:1, the in vitro drug release experiment was carried out at three different pH values, 7.4, 5 and 3. No initial burst release of gentamicin was observed in both NPs, as shown in Figures 1 and 2. The cumulative release of the gentamicin from the G-PDA NPs 1:1 at pH 5 and 3 was approx. 40% and 55%, even after 168 h, and expected to release slowly with the passage of time by maintaining its release rate, thus exhibiting a long-term release profile. On the contrary, a very slow drug-release profile (11.4%) was achieved at pH 7.4. This finding suggests the pH-dependent behavior of PDA in terms of its zwitterionic property.

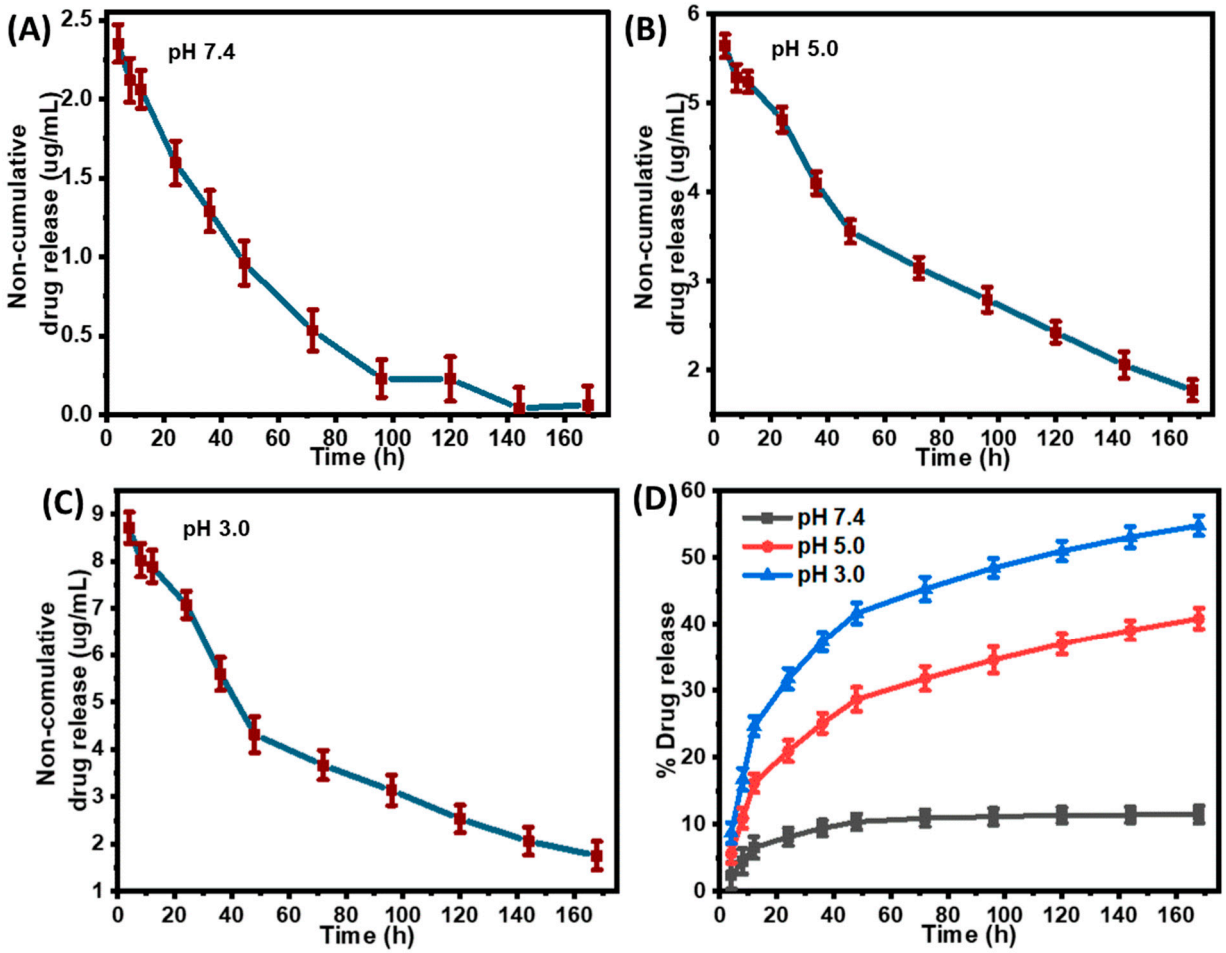

Figure 1. (**A**–**C**) are representing non-cumulative gentamicin release at pH 7.4, 5 and 3, respectively; and (**D**) is representing cumulative percent release of gentamicin at all pH conditions from G-PDA 1:1. Data were mean ± SD (n = 3).

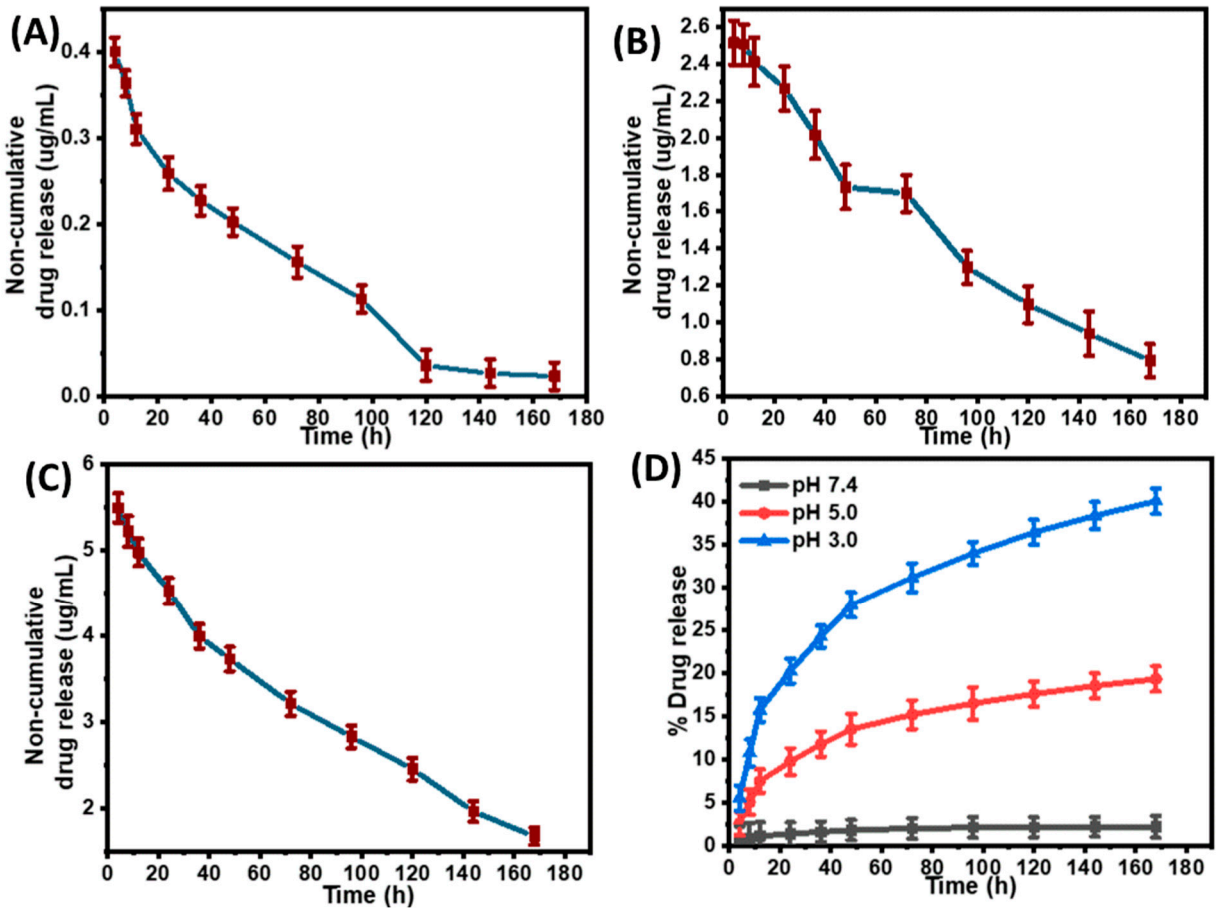

Figure 2. (**A**–**C**) are representing non-cumulative gentamicin release at pH 7.4, 5 and 3, respectively; and (**D**) is representing cumulative percent release of gentamicin at all pH conditions from G-PDA 0.6:1. Data were mean ± SD (n = 3).

Hence, the mechanism of drug release could be explained depending on the behavior of the PDA functional groups in response to pH. At an acidic pH, both the PDA NPs and gentamicin are positively charged because of the protonation of the amine groups. Thereby, the gentamicin molecules easily escape from PDA, because of the repulsive forces. Moreover, hydrogen bonding between PDA and gentamicin is also disturbed at an acidic pH, due to the interchangeable active sites of PDA resulting in gentamicin's release from the PDA NPs.

Although the G-PDA NPs 1:1 was best considered in terms of the highest possible loading efficiency as discussed in previous work, the drug release behavior for another batch of drug-loaded particles with a comparatively lower quantity of the loaded drug, i.e., G-PDA NPs 0.6:1, was studied as well. This study was performed intentionally in order to determine the effect of the loading percentage on drug release profile.

The drug release profile for the G-PDA NPs 0.6:1 was almost similar to the G-PDA NPs 1:1 with a higher drug loading amount, except for the amount of drug released during the studied time interval. The cumulative percentage of drug release after 7 days was very limited in pH 7.4, and tended towards the linear even after 40 h. It is speculated that the minor release of gentamicin at pH 7.4 was because of the excellent stability of the PDA NPs in neutral or alkaline conditions. On the other hand, at pH 5 and 3, approximately 20% and 40% of the drug had been released, respectively, showing the long-term release behavior. The concentration of drug releasing from the G-PDANPs 0.6:1 was comparatively one half of the loading amount.

In conclusion, the drug release rate of both kinds of particles at different pH values showed an insignificant difference. However, the PDA NPs with less loading amount of

gentamicin (approximately 70%) also showed a lower amount of drug release, as shown in Figure 3. On the contrary, the particles with a significantly higher loading efficiency (almost 80%) lead to a two times higher amount of drug release. It might be attributed to the fact of the concentration gradient between the two kinds of particles with different loading amounts of gentamicin.

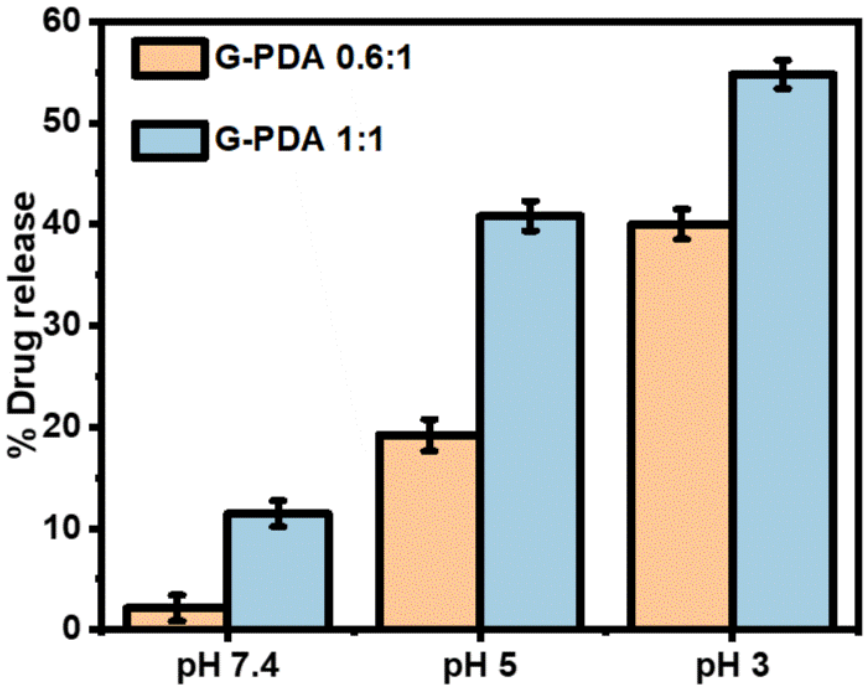

Figure 3. Comparison between % drug release from G-PDA 0.6:1 and G-PDA 1:1 at various pH conditions.

Hence, the work resulted in two different choices in terms of loading percentages and corresponding release rates for implementation in drug delivery systems. It was concluded that by tuning the feeding amount, the loading efficiency can be tuned as well as the amount of drug release, with no effect on the release profile but an effect on the drug dosage amounts.

3.3. Kinetic Study of Gentamicin Release

The implementation of mathematical models is critically important to evaluate the mechanism and kinetics of drug release from drug delivery systems. The drug release from the polymer matrix could be divided into three categories, viz.; diffusion-controlled; erosion-controlled and swelling-controlled, which are applied on non-degradable polymer and degradable and swellable polymer matrices, respectively. Table S1 (Supplementary Materials) shows various mathematical models and their mechanisms investigated so far, relating to the various drug delivery systems [31–34].

In this study, the kinetic release of gentamicin from PDA NPs was determined by employing two mathematical models, the Ritger–Peppas and Higuchi models. These models were found to be best fitted to the drug release data, supported by high correlation coefficient (R^2) values. These models suggested the diffusion-controlled release of gentamicin in response to change in pH of the environment.

The Ritger–Peppas model is represented by the following equation:

$$M_t/M_\infty = kt^n \quad (1)$$

where, M_t and M_∞ are cumulative drug release at time t and at equilibrium, respectively. M_t/M_∞ represents the fraction of drug release at time t. k is the kinetic release rate constant of the Ritger–Peppas model (h) and n is the diffusional exponent characteristic of the

release mechanism. According to the Ritger–Peppas model, the value of n demonstrates the drug release mechanism which can be divided into various categories, as described in the literature [35,36]. If $0.45 \leq n$, it corresponds to the Fickian diffusion mechanism by following Fick's law, and $0.45 < n < 0.89$ shows non-Fickian transport (anomalous diffusion). Moreover, if the value of $n = 0.89$ and $n > 0.89$, it corresponds to case II transport and super case II transport respectively. Therefore, the experimental data were plotted, and non-linear fitting was performed for the G-PDA NPs 1:1 at pH 7.4, 5 and 3 into the Ritger–Peppas model to determine the exact mechanism involved. Figures 4A, 5A and 6A show the fitting of drug release data at pH 7.4, 5 and 3, respectively, in the Ritger–Peppas model.

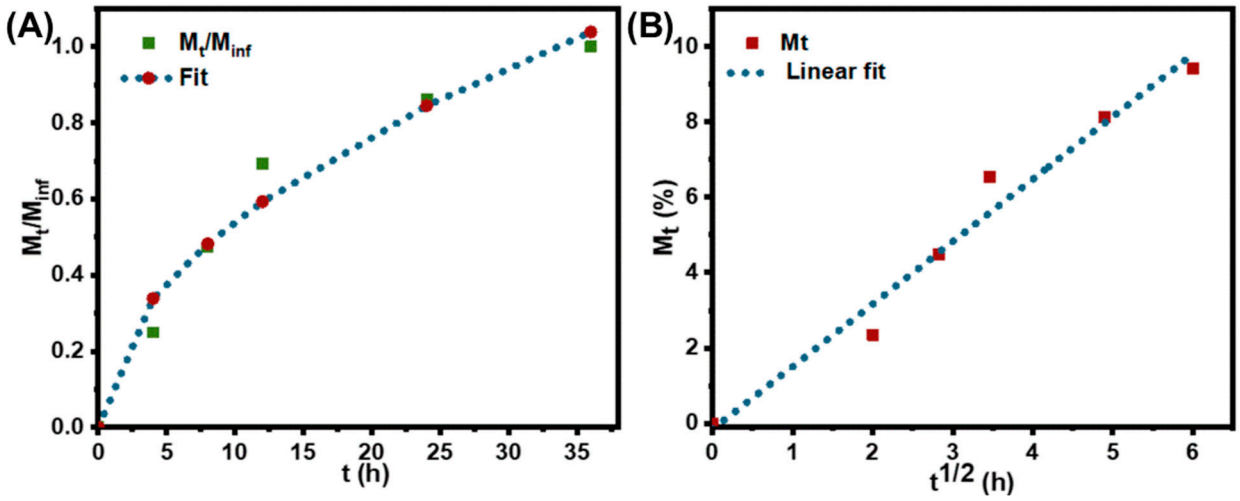

Figure 4. Fitting of cumulative % drug release data to (**A**) Ritger–Peppas and (**B**) Higuchi model for pH 7.4.

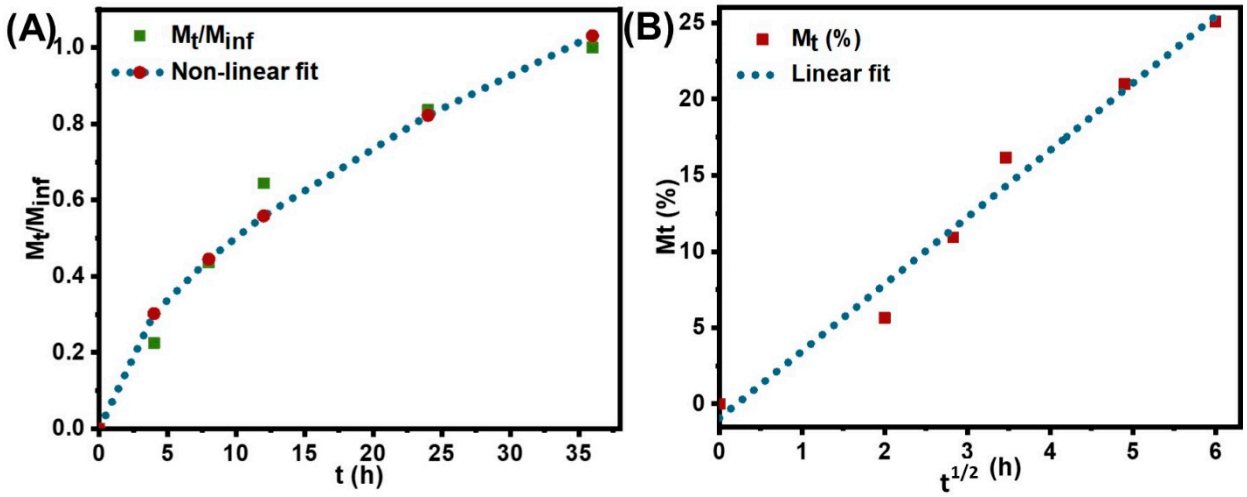

Figure 5. Fitting of cumulative % drug release data to (**A**) Ritger–Peppas and (**B**) Higuchi model for pH 5.

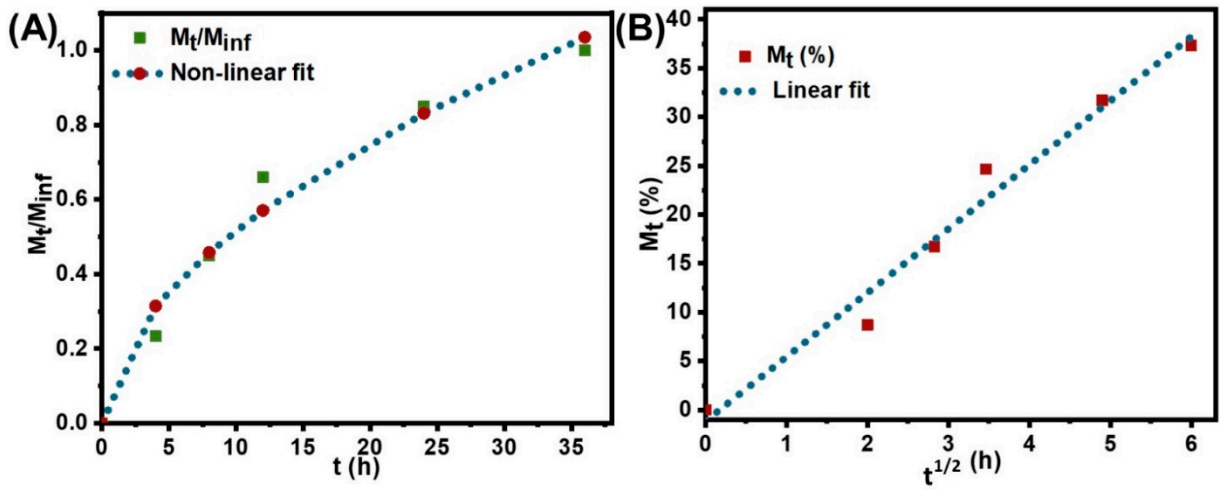

Figure 6. Fitting of cumulative % drug release data to (**A**) Ritger–Peppas and (**B**) Higuchi model for pH 3.

Please note that the Fickian diffusion is the classical diffusion process that is controlled by the concentration gradient with the constant diffusion coefficients ($0.45 \leq$ n) and relatively simple kinetic profiles of penetrant redistribution in the polymer matrix. On the other hand, in non-Fickian or anomalous diffusion, the diffusion coefficient is not constant (such as time- or concentration-dependent. Therefore, the relationship between the time and concentration changes could be because of factors such as chemical interactions between the medium and diffusant, chemical reactions, swelling and mechanical stress.

Table 2 shows various drug release parameters obtained after non-linear fitting in the Ritger–Peppas and Higuchi models. All of the particles showed the n value between 0.45 and 1, hence indicating a non-Fickian diffusion of the gentamicin from the PDA NPs. The drug release data show that the release mechanism of the gentamicin from the PDA NPs is strongly dependent on the pH of the environment which acts as a driving force for the gentamicin to diffuse from the PDA NPs to the PBS solution. Moreover, the release mechanism of the G-PDA NPs is also influenced by the structural behavior of the PDA at different pH conditions. It was previously discussed that the zwitterionic nature of PDA makes it negatively charged at alkaline pH and positively charged at acidic pH. The zwitterionic behavior is controlled by the protonation and deprotonation of the amine and hydroxyl groups, respectively. Therefore, at alkaline pH during in situ loading, its hydroxyl groups form positive–negative chemical interaction and/or hydrogen bonding with amine groups of gentamicin. Thereby, during in vitro release, the PDA structural change takes place at an acidic pH, shifting towards a positive charge, hence allowing the drug to release. This phenomenon supports the kinetic release mechanism of the G-PDA NPs which follows the non-Fickian release mechanism.

Table 2. Parameters for release kinetics obtained after fitting of Plots in Ritger−Peppas and Higuchi Models.

G-PDA 1:1	Ritger–Peppas Model			Higuchi Model	
	k	N	R^2	k_H	R^2
pH 7.4	0.1669	0.5105	0.9862	1.6571	0.9728
pH 5	0.1393	0.5586	0.9897	4.3954	0.9779
pH 3	0.1484	0.5422	0.9887	6.5609	0.9769

The diffusion-controlled drug release mechanism was also justified by the Higuchi model, which describes the drug release as a diffusion process based on square root time-dependent (Fick's law) [33,35]. This model is represented by the following equation:

$$M_t = k_H t^{1/2} \quad (2)$$

where M_t is the cumulative release (%) of the drug at time t and k_H is the kinetic release constant. The experimental data were plotted and fitted in this model, as shown in Figures 4B, 5B and 6B. It was observed that the values of kinetic release constant (k_H) are changing with the change of pH, hence supporting the pH-controlled diffusion of gentamicin from the host molecules.

4. Conclusions

In conclusion, this report sets out the detailed monitoring of in vitro gentamicin release from the G-PDA NPs in response to pH, using the dialysis method. The release test was performed for two batches with a variable gentamicin-loading amount, viz.; G-PDA NPs 1:1 and G-PDA NPs 0.6:1 at three pH conditions 3, 5 and 7.4. The PDA was found to be a stable nanocarrier in terms of drug release at an alkaline pH. The PDA, being zwitterionic in nature, provides negative active sites to chemically interact with gentamicin at a working alkaline pH. Therefore, at pH 7.4, the PDA exhibited good stability with a lower amount of gentamicin release over seven days. It is attributed to the deprotonation of the phenolic hydroxyl groups of PDA at an alkaline pH which strongly attaches to the positively charged amine groups of gentamicin. Unlike at pH 5 and 3, the amino groups of PDA are more prone towards protonation, making PDA positively charged, hence the repulsive forces cause the gentamicin to detach from its surface. Therefore, approx. 40% and 55% of the drug release was observed at pH 5 and 3, respectively. This study of gentamicin release at acidic pH was required to confirm the G-PDA NPs' behavior during local acidification caused by bacterial metabolism, hence assuring the efficacy of gentamicin. On the other hand, the G-PDA 0.6:1 with a lower loading percentage, showed a lower release under the same experimental conditions, which was attributed to the concentration gradient effect.

Two kinetic models were implemented to the drug release data, namely Ritger–Peppas and Higuchi's models, to investigate the drug release kinetics. This kinetic analysis further supported the pH-dependent drug release, hence confirming our observations, and PDA structural changes in response to pH. These findings suggested that the in situ loading method for gentamicin could provide long-term drug release over an extended period. Such an on-demand drug delivery system could be beneficial in treating various pathological tissues, meeting the drug efficacy and safety challenges.

Supplementary Materials: The following supporting information can be downloaded at: https://www.mdpi.com/article/10.3390/app12136319/s1, Figure S1. Calibration curve for gentamicin; Figure S2. C1a isomer (m/z 450.4) of gentamicin at various concentrations; Figure S3. C2/C2a isomer (m/z 464.5) of gentamicin at various concentrations; Figure S4. C1 isomer (m/z 478.5) of gentamicin at various concentrations; Table S1. Various drug release models and their mechanisms.

Author Contributions: Conceptualization, R.B. and A.Y.; methodology, R.B., M.B., A.K., A.A. and A.Y.; validation, R.B. and A.Y.; formal analysis, R.B., M.B., A.K., A.A. and A.Y.; investigation, R.B.; resources, R.B., M.B. and A.Y.; writing—original draft preparation, R.B.; writing—review and editing, M.B., A.K., A.A. and A.Y.; project administration, A.Y. All authors have read and agreed to the published version of the manuscript.

Funding: This research received no external funding.

Conflicts of Interest: The authors declare no conflict of interest.

References

1. Cooper, E.L. From Darwin and Metchnikoff to Burnet and beyond. *Contrib. Microbiol.* **2008**, *15*, 1–11. [PubMed]
2. Jain, K.K. Nanomedicine: Application of nanobiotechnology in medical practice. *Med. Princ. Pract.* **2008**, *17*, 89–101. [CrossRef] [PubMed]
3. Mudshinge, S.R.; Deore, A.B.; Patil, S.; Bhalgat, C.M. Nanoparticles: Emerging carriers for drug delivery. *Saudi Pharm. J.* **2011**, *19*, 129–141. [CrossRef] [PubMed]
4. Rana, V.; Sharma, R. Chapter 5—Recent Advances in Development of Nano Drug Delivery. In *Applications of Targeted Nano Drugs and Delivery Systems*; Mohapatra, S.S., Ranjan, S., Dasgupta, N., Mishra, R.K., Thomas, S., Eds.; Elsevier: Amsterdam, The Netherlands, 2019; pp. 93–131.
5. Torchilin, V.P. Recent advances with liposomes as pharmaceutical carriers. *Nat. Rev. Drug Discov.* **2005**, *4*, 145–160. [CrossRef]
6. Duncan, R. Polymer conjugates as anticancer nanomedicines. *Nat. Rev. Cancer* **2006**, *6*, 688–701. [CrossRef]
7. Batul, R.; Tamanna, T.; Khaliq, A.; Yu, A. Recent progress in the biomedical applications of polydopamine nanostructures. *Biomater. Sci.* **2017**, *5*, 1204–1229. [CrossRef]
8. Tran, H.Q.; Batul, R.; Bhave, M.; Yu, A. Current Advances in the Utilization of Polydopamine Nanostructures in Biomedical Therapy. *Biotechnol. J.* **2019**, *14*, e1900080. [CrossRef]
9. Liu, Y.; Ai, K.; Lu, L. Polydopamine and Its Derivative Materials: Synthesis and Promising Applications in Energy, Environmental, and Biomedical Fields. *Chem. Rev.* **2014**, *114*, 5057–5115. [CrossRef]
10. Liebscher, J. Chemistry of Polydopamine—Scope, Variation, and Limitation. *Eur. J. Org. Chem.* **2019**, *2019*, 4976–4994. [CrossRef]
11. Lee, H.; Dellatore, S.M.; Miller, W.M.; Messersmith, P.B. Mussel-inspired surface chemistry for multifunctional coatings. *Science* **2007**, *318*, 426–430. [CrossRef]
12. Schanze, K.S.; Lee, H.; Messersmith, P.B. Ten Years of Polydopamine: Current Status and Future Directions. *ACS Appl. Mater. Interfaces* **2018**, *10*, 7521–7522. [CrossRef] [PubMed]
13. Liu, Y.; Ai, K.; Liu, J.; Deng, M.; He, Y.; Lu, L. Dopamine-Melanin Colloidal Nanospheres: An Efficient Near-Infrared Photothermal Therapeutic Agent for In Vivo Cancer Therapy. *Adv. Mater.* **2013**, *25*, 1353–1359. [CrossRef]
14. Batul, R.; Yu, A.; Bhave, M.; Khaliq, A. Synthesis of Polydopamine Nanoparticles for Drug Delivery Applications. *Microsc. Microanal.* **2018**, *24* (Suppl. 1), 1758–1759. [CrossRef]
15. Ryu, J.H.; Messersmith, P.B.; Lee, H. Polydopamine Surface Chemistry: A Decade of Discovery. *ACS Appl. Mater. Interfaces* **2018**, *10*, 7523–7540. [CrossRef]
16. El Yakhlifi, S.; Ball, V. Polydopamine as a stable and functional nanomaterial. *Colloids Surf. B Biointerfaces* **2020**, *186*, 110719. [CrossRef] [PubMed]
17. d'Ischia, M.; Napolitano, A.; Ball, V.; Chen, C.-T.; Buehler, M.J. Polydopamine and Eumelanin: From Structure–Property Relationships to a Unified Tailoring Strategy. *Acc. Chem. Res.* **2014**, *47*, 3541–3550. [CrossRef] [PubMed]
18. Coskun, H.; Aljabour, A.; Uiberlacker, L.; Strobel, M.; Hild, S.; Cobet, C.; Farka, D.; Stadler, P.; Sariciftci, N.S. Chemical vapor deposition-based synthesis of conductive polydopamine thin-films. *Thin Solid Films* **2018**, *645*, 320–325. [CrossRef]
19. Yang, P.; Gu, Z.; Zhu, F.; Li, Y. Structural and Functional Tailoring of Melanin-Like Polydopamine Radical Scavengers. *CCS Chem.* **2020**, *2*, 128–138. [CrossRef]
20. Zmerli, I.; Michel, J.P.; Makky, A. Multifunctional polydopamine-based nanoparticles: Synthesis, physico-chemical properties and applications for bimodal photothermal/photodynamic therapy of cancer. *Multifunct. Mater.* **2021**, *4*, 022001. [CrossRef]
21. Jin, A.; Wang, Y.; Lin, K.; Jiang, L. Nanoparticles modified by polydopamine: Working as "drug" carriers. *Bioact. Mater.* **2020**, *5*, 522–541. [CrossRef]
22. Mavridi-Printezi, A.; Guernelli, M.; Menichetti, A.; Montalti, M. Bio-Applications of Multifunctional Melanin Nanoparticles: From Nanomedicine to Nanocosmetics. *Nanomaterials* **2020**, *10*, 2276. [CrossRef] [PubMed]
23. Zandieh, M.; Hagar, B.M.; Liu, J. Interfacing DNA and Polydopamine Nanoparticles and Its Applications. *Part. Part. Syst. Charact.* **2020**, *37*, 2000208. [CrossRef]
24. Barros, N.R.; Chen, Y.; Hosseini, V.; Wang, W.; Nasiri, R.; Mahmoodi, M.; Yalcintas, E.P.; Haghniaz, R.; Mecwan, M.M.; Karamikamkar, S.; et al. Recent developments in mussel-inspired materials for biomedical applications. *Biomater. Sci.* **2021**, *9*, 6653–6672. [CrossRef]
25. Barber, M.; Waterworth, P.M. Activity of gentamicin against Pseudomonas and hospital Staphylococci. *Br. Med. J.* **1966**, *1*, 203–205. [CrossRef]
26. Hayward, R.S.; Harding, J.; Molloy, R.; Land, L.; Longcroft-Neal, K.; Moore, D.; Ross, J.D.C. Adverse effects of a single dose of gentamicin in adults: A systematic review. *Br. J. Clin. Pharmacol.* **2018**, *84*, 223–238. [CrossRef] [PubMed]
27. Batul, R.; Bhave, M.; Mahon, P.J.; Yu, A. Polydopamine Nanosphere with In-Situ Loaded Gentamicin and Its Antimicrobial Activity. *Molecules* **2020**, *25*, 2090. [CrossRef] [PubMed]
28. Ho, C.C.; Ding, S.J. The pH-controlled nanoparticles size of polydopamine for anti-cancer drug delivery. *J. Mater. Sci. Mater. Med.* **2013**, *24*, 2381–2390. [CrossRef]
29. Zhu, Z.; Su, M. Polydopamine Nanoparticles for Combined Chemo- and Photothermal Cancer Therapy. *Nanomaterials* **2017**, *7*, 160. [CrossRef]
30. Du, C.; Qian, J.; Zhou, L.; Su, Y.; Zhang, R.; Dong, C.M. Biopolymer–Drug Conjugate Nanotheranostics for Multimodal Imaging-Guided Synergistic Cancer Photothermal–Chemotherapy. *ACS Appl. Mater. Interfaces* **2017**, *9*, 31576–31588. [CrossRef]

31. Shoaib, M.H.; Al Sabah Siddiqi, S.; Yousuf, R.I.; Zaheer, K.; Hanif, M.; Rehana, S.; Jabeen, S. Development and evaluation of hydrophilic colloid matrix of famotidine tablets. *AAPS PharmSciTech* **2010**, *11*, 708–718. [CrossRef]
32. Lin, C.C.; Metters, A.T. Hydrogels in controlled release formulations: Network design and mathematical modeling. *Adv. Drug Deliv. Rev.* **2006**, *58*, 1379–1408. [CrossRef] [PubMed]
33. Siepmann, J.; Peppas, N.A. Modeling of drug release from delivery systems based on hydroxypropyl methylcellulose (HPMC). *Adv. Drug Deliv. Rev.* **2001**, *48*, 139–157. [CrossRef]
34. Siepmann, J.; Siepmann, F. Mathematical modeling of drug delivery. *Int. J. Pharm.* **2008**, *364*, 328–343. [CrossRef] [PubMed]
35. Jain, A.; Jain, S.K. In vitro release kinetics model fitting of liposomes: An insight. *Chem. Phys. Lipids* **2016**, *201*, 28–40. [CrossRef]
36. Ritger, P.L.; Peppas, N.A. A simple equation for description of solute release I. Fickian and non-fickian release from non-swellable devices in the form of slabs, spheres, cylinders or discs. *J. Control. Release* **1987**, *5*, 23–36. [CrossRef]